Error Structure of Multiparameter Radar and Surface Measurements of Rainfall. Part III: Specific Differential Phase

V. CHANDRASEKAR

University of Alabama in Huntsville, Huntsville, Alabama

V. N. BRINGI

Colorado State University, Fort Collins, Colorado

N. BALAKRISHNAN* AND D. S. ZRNIĆ

NOAA/ERL, National Severe Storms Laboratory, Norman, Oklahoma

(Manuscript received 18 September 1989, in final form 21 February 1990)

ABSTRACT

Parts I and II of this three part paper dealt with the error structure of differential reflectivity and X-band specific attenuation in rainfall as estimated by radar and surface disdrometers. In this Part III paper we focus on the error structure of the specific differential phase (K_{DP}, °km^{-1}) measurement in rainfall. This allows us to analyze three estimators of rainfall rate, the first based on the reflectivity factor Z_H, the second based on combining reflectivity and Z_{DR}, [$R(Z_H, Z_{DR})$], and the third based on K_{DP} alone, $R(K_{DP})$. Simulations are used to model random errors in Z_H, Z_{DR} and K_{DP}. Physical variations in the raindrop size distribution (RSD) are modeled by varying the gamma parameters (N_0, D_0, m) over a range typically found in natural rainfall. Thus, our simulations incorporate physical fluctuations onto which random measurement errors have been superimposed. Radar-derived estimates of $R(Z_H, Z_{DR})$ and $R(K_{DP})$ have been intercompared using data obtained in convective rainfall with the NSSL Cimarron radar and the NCAR/CP-2 radar. As practical application of the analysis presented here, we have determined the range of applicability of the three rainfall rate estimators: $R(Z_H)$, $R(Z_H, Z_{DR})$ and $R(K_{DP})$. Our simulations show that when the rainfall rate exceeds about 70 mm h^{-1}, $R(K_{DP})$ performs better than $R(Z_H, Z_{DR})$. This result is valid over a 1 km propagation path. At intermediate rainfall rates around $20 \leqslant R \leqslant 70$ mm h^{-1}, our simulations show that $R(Z_H, Z_{DR})$ gives the least error. However, there are other reasons which make $R(K_{DP})$ useful; i.e., (i) its stability with respect to mixed phase precipitation, and (ii) the fact that it is a differential phase measurement and thus insensitive to system gain calibration. This last premise suggests an accurate method of system gain calibration based on the rain medium.

I. Introduction

Application of polarimetric techniques to the remote measurement of rainfall rate (R) is an area of continuing importance. Conventional techniques based on Z–R relations are known to introduce considerable errors when small time (~3 min) and space scales (~1 km) are considered, e.g., convective rainfall scales. In this Part III paper we discuss errors in the estimation of R using the specific differential phase measurement, i.e., the measurement that is proportional to the real part of the difference in the complex forward scatter amplitudes at horizontal (H) and vertical (V) polarizations. Seliga and Bringi (1978) first proposed that the differential propagation phase measurement could be used to determine rainfall rate, in a manner similar to that using differential reflectivity (Z_{DR}). They assumed that the differential propagation phase (ϕ_{DP}) could be measured using "fast" pulse-to-pulse switching between H and V states with corresponding copolar reception through the same receiver and processor. Mueller (1984) proposed algorithms for estimating ϕ_{DP}, one of which was analyzed by Sachidananda and Zrnić (1986) and shown to yield standard errors of about 1°–2° using 64 H and 64 V samples. Furthermore, Sachidananda and Zrnić (1989) devised a scheme to correct the ambiguities inherent in this measurement and developed formulas for simultaneously estimating Doppler spectral moments with minimum error. Jameson (1985) and Jameson and Mueller (1985) discussed the microphysical interpretation of ϕ_{DP} in rainfall assuming Rayleigh scattering (S-band

* NRC/NOAA Research Associate; permanent affiliation with Department of Aerospace Engineering, Indian Institute of Science, Bangalore 560012, India.

Corresponding author address: Dr. V. N. Bringi, Department of Electrical Engineering, Colorado State University, Fort Collins, CO 80523.

frequencies) and showed that it is proportional to the mass-weighted mean axis ratio of the oblate raindrops filling the radar resolution volume. The first measurements of ϕ_{DP} with a fast-switched radar were presented by Sachidananda and Zrnić (1987) who used the National Severe Storm Laboratory's Cimarron radar. These were followed by NCAR's CP-2 radar measurements of ϕ_{DP} taken during the summer of 1987 and reported by Golestani et al. (1989). Data from both these radars are presented in this paper.

The use of circular polarization techniques by McCormick and Hendry (1975) to estimate ϕ_{DP} predates much of the cited work based on fast-switched linear polarization. They showed that the range dependence of the complex observable W/W_2 could be used to calculate the differential propagation constant when the anisotropy axis of the medium is close to vertical, where W is the complex covariance between the two, simultaneously received circularly polarized signals, and W_2 is directly related to radar reflectivity. Data at K, X and S-bands have been presented both in rainfall and in snow (McCormick and Hendry 1974; Hendry et al. 1976; Hendry and Antar 1984). Recently, Holt (1988) showed that ϕ_{DP} may be directly obtained from S-band circularly polarized radar measurements. Data in rainfall were presented and compared with a single raingage by McGuiness and Holt (1989). Based on two cases of convective rainfall intercomparisons with a single raingage (15 min averages), they found that the ϕ_{DP} results were more stable and superior to both reflectivity and Z_{DR} methods. While these preliminary results are encouraging, it is apparent that further theoretical and experimental results are necessary before firm conclusions can be drawn. In the first two parts (I and II) of this three-part paper we concentrated on an analysis of error structure related to Z_{DR} and X-band attenuation, respectively, Chandrasekar and Bringi (1988a,b). In this Part III paper we focus on ϕ_{DP} and its range derivative termed specific differential phase, or K_{DP}.

Our paper is organized as follows. Section 2 gives a brief overview of the rain model and derived radar observables such as reflectivity, Z_{DR} and K_{DP}. Section 3 discusses the simulation of radar observables in a manner similar to that described by Chandrasekar and Bringi (1988a,b). Section 4 deals with system gain calibration and use of the properties of the rain medium to establish system bias. Section 5 describes radar data obtained with the NSSL/Cimarron and the NCAR CP-2 radars. Finally, section 6 summarizes the key results of this paper.

2. Rain model and radar observables

Ulbrich (1983) has shown that the gamma model can adequately describe many of the natural variations in the raindrop size distribution (RSD). This model has three parameters and is given by

$$N(D) = N_0 D^m \exp[-(3.67 + m)D/D_0] \quad (1)$$

where D is the volume equivalent spherical diameter and D_0 is termed the median volume diameter of the distribution. The rainfall rate $(R)^{sd}$ is defined as

$$R^{sd} = \frac{\pi}{6}\int D^3 v(D)N(D)dD, \quad \text{mm h}^{-1} \quad (2)$$

where we assume $v(D) = 17.67D^{0.67}$, a power law fit of the fall speed versus diameter relation, Atlas and Ulbrich (1977). The superscript "sd" stands for estimates based on the size distribution. The reflectivities $Z_{H,V}$ at horizontal (H) and vertical (V) polarizations, respectively, are defined as,

$$Z_{H,V} = \frac{\lambda^4}{\pi^5 |K|^2}\int \sigma_{H,V}(D)N(D)dD, \quad \text{mm}^6\,\text{m}^{-3} \quad (3)$$

where $\sigma_{H,V}(D)$ are the radar cross sections at H and V polarizations, λ is the wavelength, $K = (\epsilon_r - 1)/(\epsilon_r + 2)$, and ϵ_r is the refractive index of water. Differential reflectivity (Z_{DR}) is defined as,

$$Z_{DR} = 10\log(Z_H/Z_V), \quad \text{dB}. \quad (4)$$

The specific differential phase (K_{DP}) is defined as

$$K_{DP} = \frac{180}{\pi}\lambda\,\text{Re}\int [f_H(D) - f_V(D)]N(D)dD, \quad ^\circ\text{km}^{-1} \quad (5)$$

where f_H and f_V are the forward scattering amplitudes for horizontally (H) and vertically (V) polarized waves. The two-way differential propagation phase shift (ϕ_{DP}) is defined as

$$\phi_{DP} = 2\int_{r_1}^{r_2} K_{DP}(r)dr \quad (6)$$

where r_1 and r_2 are ranges from the radar. Note that Sachidananda and Zrnić (1986) have defined K_{DP} as twice the value given by Eq. (5). We use the definition here because it is conventional in the propagation literature.

The equilibrium shapes of raindrops have been studied extensively [Pruppacher and Klett (1978)]. Recently, computations using a new model were reported by Beard and Chuang (1987). Experimentally derived axis ratios of raindrops using imaging probes have been reported by Chandrasekar et al. (1988c). Fig. 1 shows the axis ratio, b/a (b and a are the semiminor and semimajor axes, respectively) as a function of D for two cases; (i) Green's (1975) equilibrium formula, and (ii) as derived from the average experimental results of Chandrasekar et al. (1988c). The sensitivity of Z_{DR} to these two axis ratio relations has been calculated by Chandrasekar et al. (1988) for an exponential RSD [$m = 0$ in Eq. (1)] showing that a difference

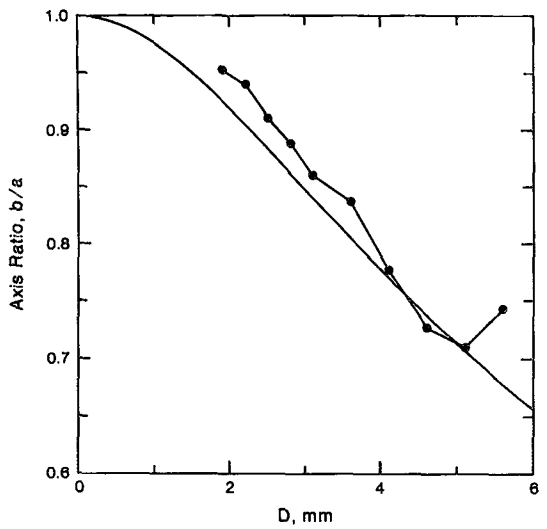

FIG. 1. Axis ratio, b/a, versus volume equivalent spherical diameter D. The solid line is based on Green's (1975) formula for equilibrium shapes. The dots refer to axis ratio estimates derived from 2D-PMS probe images of raindrops. Figure adapted from Chandrasekar et al. (1988c).

of, at most, 0.3 dB in Z_{DR} may be expected between the two relations for $1 \leq D_0 \leq 3$ mm.

The radar rainfall rate estimation techniques considered here are based on (i) the combination of Z_H with Z_{DR}, and (ii) K_{DP} alone. Sachidananda and Zrnić (1987) have given a $R(K_{DP})$ relation of the form,

$$R(K_{DP}) = 37.1(K_{DP})^{0.866}, \quad \text{mm h}^{-1} \qquad (7)$$

which is derived for a Marshall–Palmer (1948) RSD and equilibrium axis ratios. Chandrasekar and Bringi (1988a) derived a $R(Z_H, Z_{DR})$ relation of the form $R(Z_H, Z_{DR}) = FZ_H^{\alpha}Z_{DR}^{\beta}$ where R is in mm h^{-1}, Z_H is in mm^6 m^{-3} and Z_{DR} in dB. We obtained the best fit values of F, and α and β by first varying the gamma RSD parameters N_0, m and D_0 over the following ranges, $10^{4.2}\exp(2.8m) \leq \text{No} \leq 10^{5.5}\exp(3.57m)$, $\text{m}^{-3}\,\text{mm}^{-1-m}$, $0 < D_0 \leq 2.5$ mm, $-1 < m \leq 4$, Ulbrich (1983). These parameters were randomly varied over their respective ranges with maximum drop diameter, $D_m = 8$ mm. R^{sd}, Z_H and Z_{DR} are computed using Eqs. 2, 3, and 4 for each triplet of points (N_0, D_0, m) using Green's (1975) axis ratios. A nonlinear regression is performed to find the best-fit F, α and β resulting in

$$R(Z_H, Z_{DR}) = 1.98 \times 10^{-3}Z_H^{0.97}Z_{DR}^{-1.05}, \quad \text{mm h}^{-1} \qquad (8)$$

Note that the value of β obtained here differs from earlier results of Aydin et al. (1987) who obtained $\beta = -1.67$, and Ulbrich and Atlas (1984) who obtained $\beta = -1.50$, with corresponding $\alpha = 1$.

A similar procedure for K_{DP} was performed and the nonlinear regression of the form $R(K_{DP}) = CK_{DP}^{\alpha}$ yielded

$$R(K_{DP}) = 40.5(K_{DP})^{0.85} \qquad (9)$$

which is in excellent agreement with Eq. 7. It turns out that Eq. (8) is robust with respect to variations in both D_m and axis ratio. For example, when D_m was decreased from 8 to 6 mm, keeping all other assumptions the same, the best-fit F, α and β were nearly the same as those given by Eq. (8). If the axis ratio variation is changed from Green (1975) to the experimentally derived ones (see Fig. 1), the best-fit F, α and β were, respectively, 1.94×10^{-3}, 0.97, 1.044. The reason that F, α and β are robust is because of the way in which Z_H and Z_{DR} are combined; i.e., when D_m decreases, both Z_H and Z_{DR} decrease together in such a way that the final best-fit values are not significantly altered. Sachidananda and Zrnić (1987) show that $R(K_{DP})$ is not sensitive to D_m variations. However, it is sensitive to axis ratio variations; e.g., our procedure when applied to the experimental axis ratios yielded best-fit C and α to be, respectively, 56 and 0.8.

Figures 2a,b show scatterplots of $R(Z_H, Z_{DR})$ versus R^{sd} and $R(K_{DP})$ versus R^{sd}, respectively, where each data point was obtained from one triplet of gamma parameters (N_0, D_0, m). Here $R(Z_H, Z_{DR})$, $R(K_{DP})$, and R^{sd} are obtained by using Eqs. (8), (9), and (2). The scatter is representative of natural variations in the RSD to the extent that RSDs can be parameterized by the gamma form, Ulbrich (1983). Chandrasekar and Bringi (1988a) showed a similar scatterplot of $R(Z_H)$ versus R^{sd} which differs from Fig. 2 in two respects: (i) a significant bias is present for $R^{sd} \geq 20$ mm h^{-1} and (ii) the variance for $R^{sd} \geq 20$ mm h^{-1} is much larger. Note that they obtained $R(Z_H)$ from $Z_H = 200R^{1.6}$. Figure 2 shows that the estimation of rainfall rate using $R(Z_H, Z_{DR})$ and $R(K_{DP})$ under ideal conditions introduces small error as a result of gamma parameter fluctuations in the ranges described earlier.

Surface disdrometers and aircraft PMS (Particle Measuring Systems, Inc.) probes are widely used to sample the RSD. Thus, it is instructive to estimate the sampling errors in K_{DP} in a manner similar to that described by Chandrasekar and Bringi (1988a) for Z_{DR}. This procedure and related disdrometer data are given in Appendix A.

3. Simulation of radar observables

Radar measurements of Z_H and Z_{DR} involve estimation of the mean backscattered powers, whereas the ϕ_{DP} measurement involves "pulse-pair" type algorithms for estimation of differential phase shifts (Doviak and Zrnić 1984; Zrnić 1979; Sachidananda and Zrnić 1986). Fluctuations in these estimates can be related to the width (σ_v) of the Doppler spectrum. Zrnić (1975) has developed a procedure for simulating univariate signal samples assuming a Gaussian form for the Doppler spectrum. Chandrasekar et al. (1986) generalized this procedure to simulate a bivariate time

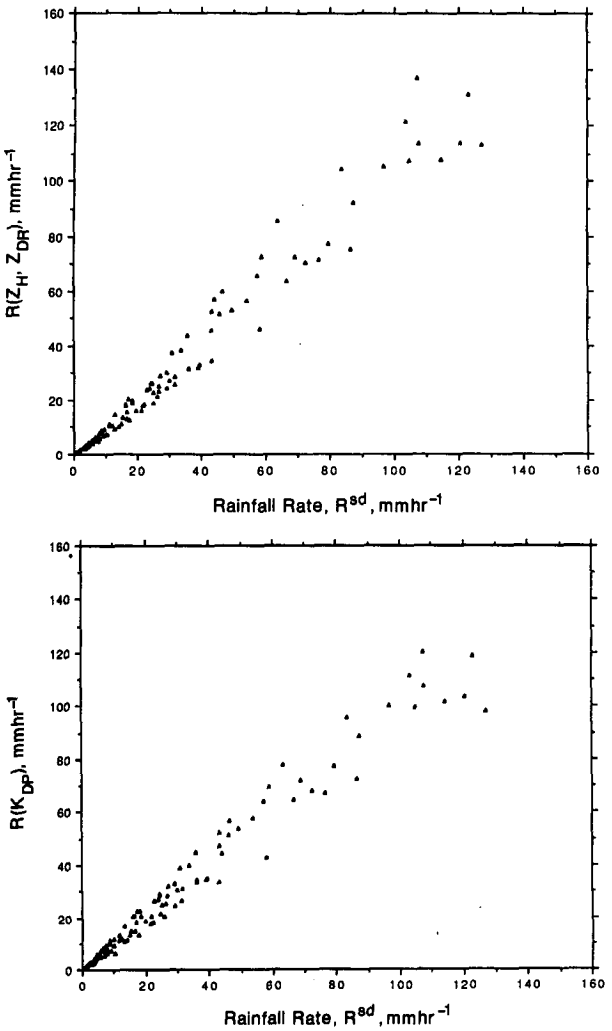

FIG. 2. Scatterplot of (a) $R(Z_H, Z_{DR})$ and (b) $R(K_{DP})$ versus rainfall rate R^{sd}, where each data point refers to one value of the triplet of parameters (N_0, D_0, m) of the gamma distribution. $R(Z_H, Z_{DR})$, $R(K_{DP})$, and R^{sd} are computed using Eqs. (8), (9) and (2), respectively.

series from which Z_{DR} could be estimated. The same bivariate signals can also be used to estimate ϕ_{DP} using Mueller's (1984) algorithm. The dual polarized signals having the same Doppler spectrum are independently simulated at two ranges, r_1 and r_2. The propagation path is defined to be the range interval $(r_2 - r_1)$ which is characterized by a constant K_{DP}. The simulated mean $\phi_{DP}(r_2)$ is obtained from mean $\phi_{DP}(r_1)$ by adding $2K_{DP}(r_2 - r_1)$. From the simulated ϕ_{DP} range profile, K_{DP} can be estimated using a simple finite difference scheme for slope estimation, or by more sophisticated schemes as described by Golestani et al. (1989) and Zrnić et al. (1989).

The principal assumptions are as follows:

- Gaussian Doppler spectrum with σ_v varying between 1 and 6 m s^{-1} in proportion to reflectivity,
- 128 samples at each polarization,
- Pulse repetition time of 1 ms,
- Radar wavelength of 10 cm,
- Zero-lag cross-correlation (ρ_{HV}) of 0.99, and
- The simulated fluctuations in K_{DP} are equivalent to those obtained using a least-squares fit to the ϕ_{DP} profile over a propagation path of 1 km having 7 range samples.

Our simulation also models random errors in Z_H, Z_{DR}, and K_{DP}. Physical fluctuations in the RSD are introduced by varying the gamma parameters N_0, D_0, m over the wide range specified in section 2.

We now define the following variables where the superscript "sm" stands for simulation:

Z_H^{sm}	Estimate of reflectivity from radar simulations.
Z_{DR}^{sm}	Estimate of differential reflectivity from radar simulations.
K_{DP}^{sm}	Estimate of K_{DP} from radar simulations.
$R^{sm}(Z_H, Z_{DR})$	Estimate of rainrate obtained using Z_H^{sm} and Z_{DR}^{sm} in Eq. (8).
$R^{sm}(K_{DP})$	Estimate of rainrate obtained using K_{DP}^{sm} in Eq. (9).

For a given triplet of gamma parameters (N_0, D_0, m) we compute R^{sd} using Eq. (2), as well as Z_H, Z_{DR} and K_{DP} using Eqs. (3), (4) and (5), respectively, which correspond to the mean radar observables. Radar simulations are used to calculate Z_H^{sm}, Z_{DR}^{sm}, and K_{DP}^{sm} from which $R^{sm}(Z_H, Z_{DR})$ and $R^{sm}(K_{DP})$ are obtained. This process is repeated for each (N_0, D_0, m) triplet. Figures 3a,b show scatterplots of $R^{sm}(Z_H, Z_{DR})$ versus R^{sd} and $R^{sm}(K_{DP})$ versus R^{sd}. These figures incorporate physical RSD fluctuations onto which random measurement errors have been superimposed, and they can be compared with Figs. 2a,b. Figure 3c shows the scatterplot of $R^{sm}(Z_H, Z_{DR})$ versus $R^{sm}(K_{DP})$ which is the type of data that can be realized in practice. Similar radar measurements will be shown in the next section. Comparing Figs. 3a,b we see that $R^{sm}(Z_H, Z_{DR})$ performs "better," i.e., has less scatter than $R^{sm}(K_{DP})$ when $R^{sd} \leqslant 70$ mm h^{-1}. We note here that the standard error of the K_{DP} estimate decreases as the propagation path over which ϕ_{DP} is measured is increased. Our simulations are valid for a 1 km path which is appropriate for convective rainfall scales. However, the path cannot be increased indefinitely because averaging may then include inhomogeneous precipitation. Figure 3b shows that, for a given propagation path, the fractional standard deviation of the $R^{sm}(K_{DP})$ estimate will vary inversely with rainfall rate. However, the fractional standard deviation of $R^{sm}(Z_H, Z_{DR})$ does not significantly decrease with rainfall rate. Since the fractional standard deviation of $R^{sm}(K_{DP})$ estimate decreases with increasing rainrate, the region where the scatter in $R^{sm}(K_{DP})$ and $R^{sm}(Z_H, Z_{DR})$ are comparable in chosen

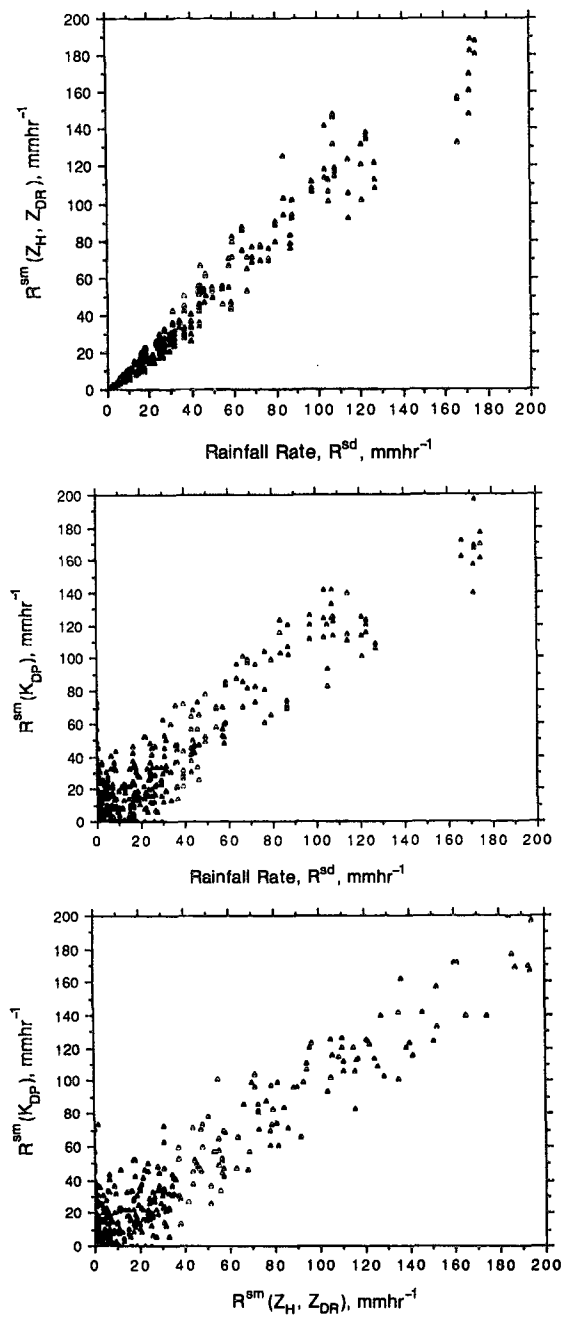

FIG. 3. Scatterplot of (a) $R^{sm}(Z_H, Z_{DR})$ and (b) $R^{sm}(K_{DP})$ versus R^{sd}. Each data point refers to one triplet of gamma parameters (N_0, D_0, m) onto which random measurement errors have been superimposed. (c) Scatterplot of $R^{sm}(K_{DP})$ versus $R^{sm}(Z_H, Z_{DR})$.

visually as being approximately 70 mm h^{-1}. Further discussion of the range of applicability of $R(Z_H)$, $R(Z_H, Z_{DR})$ and $R(K_{DP})$ is given in section 6.

4. System gain calibration

Conventional techniques for system gain calibration include use of a metallic sphere as a standard target of known radar cross section, the use of the sun as a standard source of noise power, and far-field techniques using standard gain horns. Here we follow a procedure similar to that given by Aydin et al. (1983) to evaluate the use of the rain medium itself for accurate system gain calibration. The method assumes that Z_{DR} can be accurately calibrated because it is a differential power measurement, and raindrops at vertical incidence form good, standard, beam-filling targets for which Z_{DR} is 0 dB. Since K_{DP} is obtained from relative phase measurements, it is unaffected by system gain calibration. The differential phase shift due to backscatter that could potentially affect K_{DP} is negligible at S-band (Jameson 1985). The technique involves comparing $R(Z_H, Z_{DR})$ with $R(K_{DP})$ in rainfall, and noting any systematic deviation from the 1:1 line. Any observed deviation can then be removed by appropriately adjusting the system gain (or equivalently Z_H). Figure 4a shows $R(Z_H, Z_{DR})$ versus $R(K_{DP})$ for gamma RSDs which is obtained from Fig. 2. Note that the scatter, as expected, is evenly distributed about the 1:1 line. A 2 dB bias (positive) in Z_H is introduced and the resulting scatterplot of $R(Z_H, Z_{DR})$ versus $R(K_{DP})$ is shown in Fig. 4b. Note that the scatter systematically deviates above the 1:1 line. Similarly, for a negative bias in Z_H the scatter will systematically deviate below the 1:1 line. In practice such biases can be estimated to within ±1 dB by ensuring that radar measurements of $R(Z_H, Z_{DR})$ and $R(K_{DP})$ are evenly scattered about the 1:1 line. The achievable accuracy is possibly limited by the sensitivity of $R(K_{DP})$ to the axis ratio versus diameter relationship as discussed in section 2.

5. Radar measurements

We report on radar measurements collected by the S-band NSSL/Cimarron radar and the NCAR/CP-2 radar. The main characteristics of these radars are described by Keeler et al. (1989), Carter et al. (1986), and Bringi and Hendry (1989). For both radars ϕ_{DP} is estimated by using time-series data which poses a limit on the amount and extent of data that can be gathered.

The NSSL/Cimarron radar data were obtained on 10 June 1986 in a convective rainshaft between the ranges of 38 and 62 km. The radar was performing sector scans at a fixed elevation angle of 1° with range samples spaced at 150 m intervals. Range profiles of ϕ_{DP} were constructed and a least-squares fit over a 1 km path was used to estimate K_{DP} at the center of the 1 km path. Figure 5a shows $R(Z_H, Z_{DR})$ versus $R(K_{DP})$. Above 40 mm h^{-1}, a bias in Z_H of 0.45 dB was determined. Data at lower rainrates were not included because $R(K_{DP})$ is noisy. In comparing Fig. 5a and 3c we observe qualitatively that the scatter is similar, one indication that the simulation technique discussed in section 3 is "realistic."

The CP-2 radar data were obtained near Boulder,

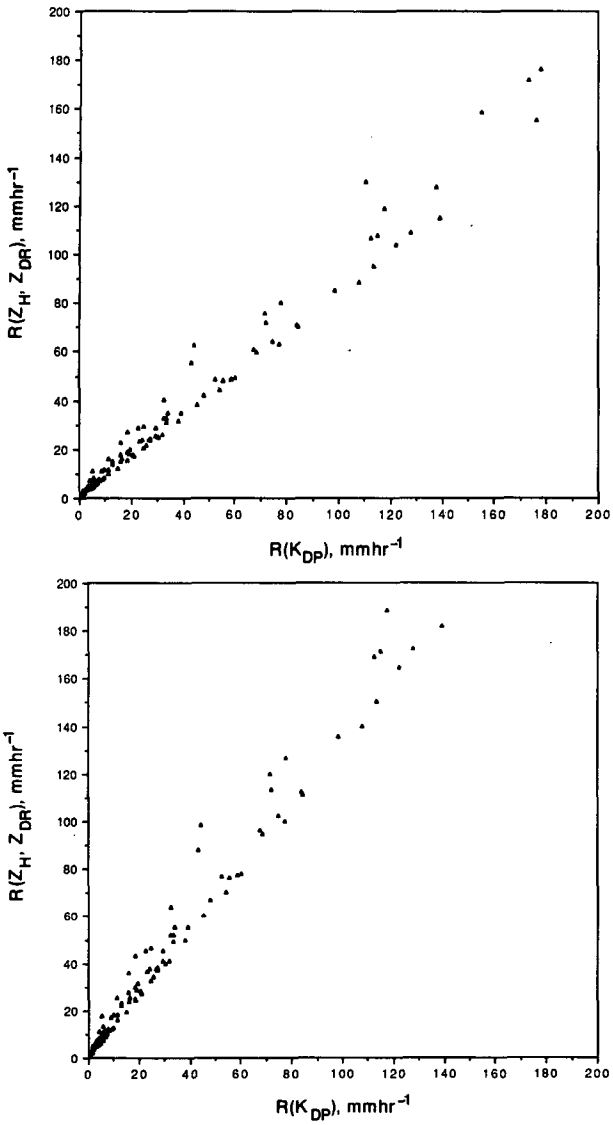

FIG. 4. Scatterplot of (a) $R(Z_H, Z_{DR})$ versus $R(K_{DP})$ assuming no systematic error in Z_H. (b) As in (a) except a 2 dB bias in Z_H is introduced. Each data point refers to one value of the triplet of gamma parameters (N_0, D_0, m).

Colorado during the summer of 1987. Data from several convective storms have been pooled together. Range profiles of Z_H, Z_{DR}, and ϕ_{DP} were individually examined. The Z_H and Z_{DR} fields were filtered in range using a weighted, moving average filter. A nondecreasing third-order polynomial was fitted to the ϕ_{DP} profile and K_{DP} was subsequently estimated at each gate using the procedure described in Golestani et al. (1989). Figure 5b shows the mean value of $R(Z_H, Z_{DR})$ averaged over 5 mm h^{-1} bin categories of $R(K_{DP})$. A bias in Z_H of 2 dB has been removed. The vertical bars represent the standard deviation about the mean $R(Z_H, Z_{DR})$, i.e., the sample standard deviation. In a qualitative sense, these deviations compare favorably with the scatter shown in Fig. 3c.

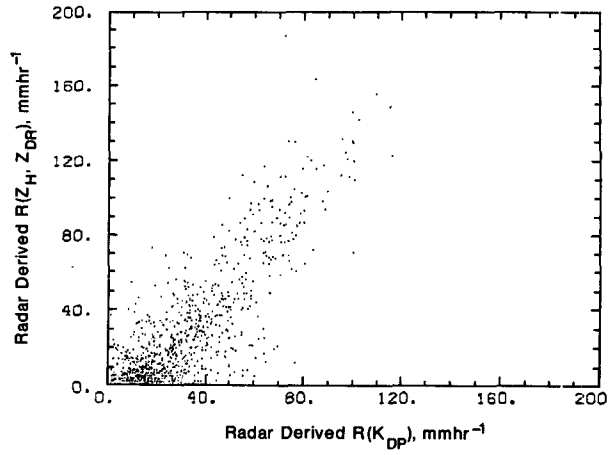

FIG. 5a. Radar derived rainfall rates using the NSSL/Cimarron radar. Z_H, Z_{DR}, and K_{DP} are derived from time series observations in convective rainshafts. $R(Z_H, Z_{DR})$ and $R(K_{DP})$ are computed using measured values of Z_H, Z_{DR}, and K_{DP} in Eqs. (8) and (9), respectively.

6. Summary and conclusions

In this Part III paper we have studied rainfall rate estimators $R(Z_H, Z_{DR})$ and $R(K_{DP})$. Random measurement errors, as well as natural fluctuations in the raindrop size distribution, were simulated to investigate the error structure of $R(Z_H, Z_{DR})$ and $R(K_{DP})$. A technique for system gain calibration based on the rain medium is proposed. It uses the intercomparison of $R(Z_H, Z_{DR})$ versus $R(K_{DP})$. Radar data in convective rainshafts from the NSSL Cimarron radar and the NCAR/CP-2 radar were presented and shown to be in good agreement with simulation results.

A practical application of the analyses presented here is to determine the range of applicability of the three formulas for rainfall rate, i.e., $R(Z_H)$, $R(Z_H, Z_{DR})$,

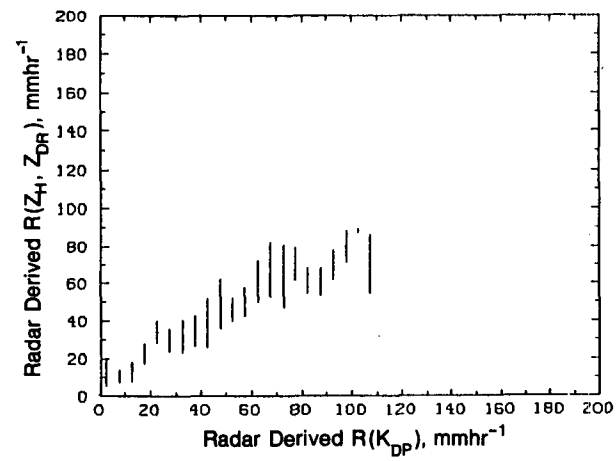

FIG. 5b. Radar derived rainfall rates using the NCAR/CP-2 radar. Z_H, Z_{DR}, and K_{DP} are derived from time series observations in convective rainshafts. $R(Z_H, Z_{DR})$ and $R(K_{DP})$ are calculated using measured Z_H, Z_{DR}, and K_{DP} in Eqs. (8) and (9), respectively. The mean value of $R(Z_H, Z_{DR})$ is computed over 5 mm h^{-1} bin categories of $R(K_{DP})$. The vertical bars represent the sample standard deviation.

and $R(K_{DP})$, giving due consideration to random measurement errors as well as physical variations of the RSD. In the Part I paper, Chandrasekar and Bringi (1988a) concluded that $R(Z_H, Z_{DR})$ does not significantly outperform $R(Z_H)$ based on Marshall–Palmer (1948) when $R \leqslant 20$ mm h^{-1}, the reason is that the random error in Z_{DR} masks any improvement obtained by the extra information provided by Z_{DR}. However, extensive space–time averaging could improve the $R(Z_H, Z_{DR})$ estimates at low rainrates, as shown by Aydin et al. (1987). Our simulations and measurements show that $R(K_{DP})$ is noisy at low rainrates. At high rainrates, our simulations indicate that $R(K_{DP})$ should outperform $R(Z_H, Z_{DR})$ since the fractional standard deviation of the $R(K_{DP})$ estimate varies inversely with rainrate, whereas for $R(Z_H, Z_{DR})$ the fractional standard deviation does not decrease significantly with rainrate. There appears to be an intermediate range where $R(Z_H, Z_{DR})$ gives the least error. The upper limit of this range depends on the propagation path and the homogeneity of the precipitation over this path, and hence a unique specification of this upper limit is subjective. Our simulations over a 1 km path show this upper limit to be around 70 mm h^{-1}. There are other reasons that make $R(K_{DP})$ useful, mainly its stability with respect to mixed phase precipitation frequently observed in convective storms (Zrnić et al. 1989). In other words, $R(K_{DP})$ will yield better estimates of rainrate than $R(Z_H)$ or $R(Z_H, Z_{DR})$ when the precipitation is a mixture of raindrops and hail. The other important reason is that $R(K_{DP})$ is a differential phase measurement, and therefore insensitive to system gain calibration.

Acknowledgments. Two of the authors, V. Chandrasekar and V. N. Bringi, acknowledge support through the Army Research Office's Center for Geosciences at Colorado State University. The authors acknowledge the assistance of Mr. Y. Golestani in processing the CP-2 radar data, and the central role played by Mr. Grant Gray of NCAR in the time series data collection. N. Balakrishnan and D. Zrnić acknowledge dedicated efforts of the NSSL engineering staff led by D. Sirmans that made modifications to the radar; M. Schmidt and C. Clark operated the radar during data collection. Part of the work performed by NSSL scientists was supported by the Joint System Program Office of the National Weather Service.

APPENDIX A

Standard Error in the Estimate of K_{DP} from Disdrometer

In raindrop sampling devices such as disdrometers, the measurement variability is due to both statistical sampling errors and very fine-scale physical variations that are not readily separate from statistical ones. Gertzman and Atlas (1977) have obtained the variance of sample moments of RSD like Z and R, whereas Chandrasekar and Bringi (1988a,b) derived the correlation between the parameter estimates. They have also obtained the standard error in the measurement of Z_{DR} derived from disdrometer samples of the RSD. In this section we obtain the accuracy of K_{DP} obtained from disdrometer samples of the RSD.

Let $D_1, D_2, \ldots, D_n$ be the diameters of the raindrops sampled by a disdrometer with fixed sample volume V, where (n) is the total number of drops observed. Then the disdrometer estimate of K_{DP} can be written as

$$\hat{K}_{DP} = \frac{180}{\pi} \cdot \frac{1}{V} \cdot \sum_{i=1}^{n} [f_H(D_i) - f_V(D_i)]. \quad \text{(A1)}$$

It can be easily shown that this estimator for K_{DP} is unbiased.

The variance of K_{DP} can be written as,

$$\text{var}(\hat{K}_{DP}) = E(n) \cdot \left(\frac{180}{\pi}\right)^2 \times E\{\text{Re}[f_H(D_i) - f_V(D_i)]\}^2, \quad \text{(A2)}$$

where the symbole $E(\ )$ stands for expectation and $E(n)$ is the mean number of drops sampled and can be written as

$$E(n) = \frac{VN_0\Gamma(m+1)}{\Lambda^{m+1}}. \quad \text{(A3)}$$

The second expectation $E(\ )$ is computed over the raindrop size distribution for the equilibrium shapes of raindrops.

The fractional standard deviation FSD of K_{DP} can be obtained from Eqs. A1, A2, and A3 as

$$\text{FSD}(K_{DP}) = \frac{\sigma(K_{DP})}{K_{DP}} = \frac{1}{\sqrt{E(n)}} \times \frac{[E\{\text{Re}[f_H(D_i) - f_V(D_i)]\}^2]^{1/2}}{E\{\text{Re}[f_H(D_i) - f_V(D_i)]\}} \quad \text{(A4)}$$

$$\sigma(K_{DP}) = [\text{var}(\hat{K}_{DP})]^{1/2}. \quad \text{(A5)}$$

Figure A1 shows $\sqrt{N_s}\,\text{FSD}(K_{DP})$ plotted as a function of median diameter D_0 with m as parameter where N_s is the mean number of drops sampled by the disdrometer. The decrease of FSD with increasing D_0 and m can be primarily attributed to the increase in K_{DP}. For the same number of drops sampled, K_{DP} will be higher for a larger D_0 and m than for a smaller D_0 and m. This feature is predominantly exhibited in the curves of the FSD.

Figure A2 shows similar results obtained from disdrometer samples. The ordinate represents the fractional standard deviation of K_{DP} multiplied by $\sqrt{N_s}$ where N_s is the number of drops sampled by the disdrometer. The abscissa is the median drop diameter. The scattergram was obtained from disdrometer data collected during the summer of 1987 at Norman,

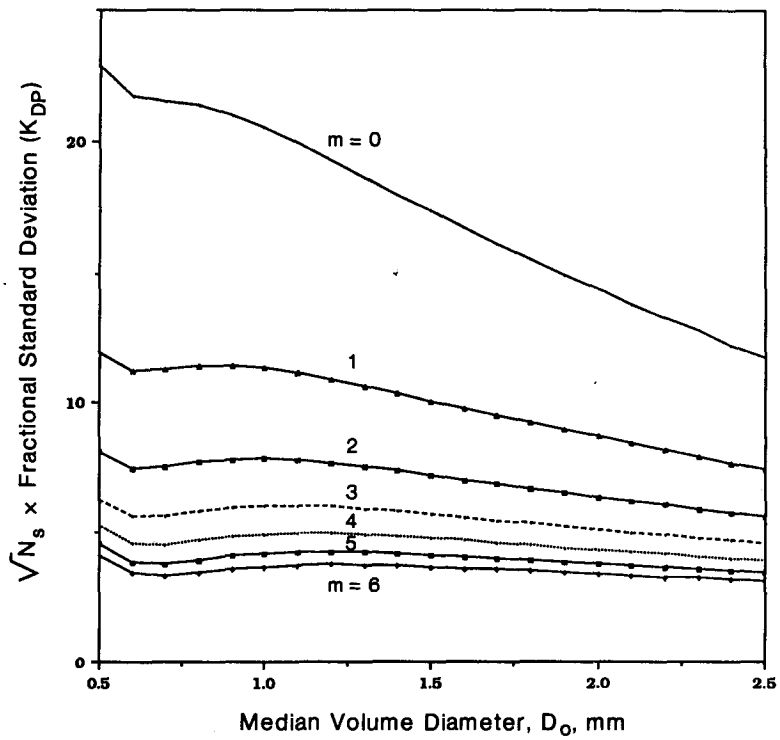

FIG. A1. Theoretical computations of $\sqrt{N_s} \times$ fractional standard deviation (K_{DP}) versus the median volume diameter D_0 for a gamma raindrop size distribution. N_s is the number of sampled raindrops. The parameter (m) reflects the shape and breadth of the gamma distribution.

Oklahoma. More details can be found in Balakrishnan et al. (1989). All the K_{DP} values calculated from the disdrometer were grouped into 0.1 mm bin categories of D_0 computed from the disdrometer samples. The standard deviation of these grouped K_{DP} is evaluated and shown in Fig. A2. We recognize that the standard deviation shown in Fig. A2 could have some component of physical variability together with the experimental fluctuations of K_{DP} measurements. However, the computed standard errors in measurements falls within the range of values predicted by the theoretical curves given in Fig. A1, thus verifying the theoretical results of fractional standard error in K_{DP} obtained from a disdrometer.

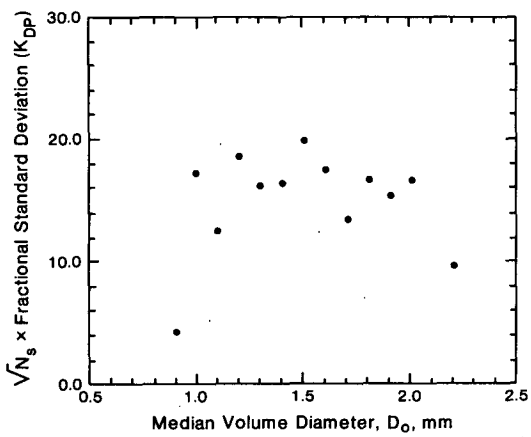

FIG. A2. As in Fig. A1 except solid dots obtained from disdrometer samples of raindrop size distributions. Disdrometer located in Norman, Oklahoma.

The theoretical analysis presented here assumes a uniform sampling volume independent of the diameter. However, in a disdrometer the sampling volume changes with size. The method of handling situations where the sampling volume varies with size is given in Chandrasekar and Bringi (1988).

REFERENCES

Atlas, D., and C. W. Ulbrich, 1977: Path- and area-integrated rainfall measurement by microwave attenuation in the 1–3 cm band. *J. Appl. Meteor.*, **16**, 1322–1331.

Aydin, K., H. Direskeneli and T. A. Seliga, 1987: Dual-polarization radar estimation of rainfall parameters compared with ground-based disdrometer measurements: October 29, 1982 Central Illinois experiment. *IEEE Trans. Geosci. Remote Sens.*, **25**(6), 834–844.

——, T. A. Seliga, C. P. Cato and M. Arai, 1983: Comparison of measured X-band reflectivity factors with those derived from S-band measurements at horizontal and vertical polarizations. Preprints, *21st Conf. Radar. Meteorology*, Edmonton, Amer. Meteor. Soc., 513–517.

——, ——, J. Goldhirsh and J. Rowland, 1989: Comparison of simulated rain rates from disdrometer data employing polarimetric radar algorithms, *J. Atmos. Oceanic Technol.*, **6**, 476–486.

Beard, K. V., and D. Chuang, 1987: A new model for the equilibrium shapes of raindrops. *J. Atmos. Sci.*, **44**, 1509–1524.

Bringi, V. N., and A. Hendry, 1989: Technology of polarization diversity radars for meteorology, Chapter 19a, *Radar in Meteorology,* D. Atlas, Ed. Amer. Meteor. Soc., in press.

Carter, J. K., D. Sirmans and J. Schmidt, 1986: Engineering description of the NSSL dual linear polarization Doppler weather radar. Preprints, *23rd Conf. on Radar Meteorology,* Vol. 3, Snowmass, Amer. Meteor. Soc., JP381–384.

Chandrasekar, V., and V. N. Bringi, 1988a: Error structure of multiparameter radar and surface measurements of rainfall. Part I: Differential reflectivity. *J. Atmos. Oceanic Technol.*, **5**, 783–795.

——, and ——, 1988b: Error structure of multiparameter radar and surface measurements of rainfall. Part II: X-band attenuation. *J. Atmos. Oceanic Technol.*, **5**, 796–802.

——, ——, and P. J. Brockwell, 1986: Statistical Properties of Dual-Polarized Radar Signals, Preprints, *23rd Conf. Radar Meteorology,* Vol. 1, Snowmass, Amer. Meteor. Soc., 193–196.

——, W. A. Cooper and V. N. Bringi, 1988c: Axis ratios and oscillations of raindrops, *J. Atmos. Sci.*, **44**(8), 1323–1333.

Doviak, R. J., and D. S. Zrnić, 1984: *Doppler Radar and Weather Observations.* Academic Press, 458 pp.

Gertzman, H. S., and D. Atlas, 1977: Sampling errors in the measurement of rain and hail parameters. *J. Geophys. Res.*, **82**(31), 4955–4966.

Green, A. W., 1975: An approximation for the shapes of large raindrops. *J. Appl. Meteor.*, **14**, 1578–1583.

Golestani, Y., V. Chandrasekar and V. N. Bringi, 1989: Intercomparison of multiparameter radar measurements. Preprints, *24th Conf. Radar Meteorology,* Tallahassee, Amer. Meteor. Soc., 309–314.

Hendry, A., and Y. M. M., Antar, 1984: Precipitation particle identification with centimeter wavelength dual-polarization radar. *Radio Sci.*, **19**(1), 115–122.

——, G. C. McCormick and B. L. Barge, 1976: KU-band and S-band observations of the differential propagation constant in snow. *Trans. IEEE,* AP-24, **4**, 521–525.

Holt, A. R., 1988: Extraction of differential propagation phase from data from S-band circularly polarized radars. *Electron. Lett.*, **24**, 1241–1242.

Jameson, A. R., 1985: Microphysical interpretation of multiparameter radar measurements in rain. Part III: Interpretation and measurement of propagation differential phase shift between orthogonal linear polarizations. *J. Atmos. Sci.*, **42**, 607–614.

——, and E. A. Mueller, 1985: Estimation of propagation differential phase shift from sequential orthogonal linear polarization radar measurements. *J. Atmos. Oceanic Technol.*, **2**, 133–137.

Keeler, R. J., B. W. Lewis and G. R. Gray, 1989: Description of NCAR/FOF CP-2 Meteorological Doppler radar. Preprints, *24th Conf. Radar Meteorology,* Tallahassee, Amer. Meteor. Soc., 589–592.

Marshall, J. S., and W. Mc. K. Palmer, 1948: The distribution of raindrops with size. *J. Meteor.*, **5**, 165–166.

McCormick, G. C., and A. Hendry, 1974: Polarization properties of transmission through precipitation over a communication link. *J. Rech. Atmos.*, **8**(1–2), 175–187.

——, and ——, 1975: Principles for the radar determination of the polarization properties of precipitation. *Radio Sci.*, **10**(4), 421–434.

McGuiness, R., and A. Holt, 1989: The extraction of rain rates from CDR data. Preprints, *24th Conf. Radar Meteorology,* Tallahassee, Amer. Meteor. Soc., 338–341.

Mueller, E. A., 1984: Calculation procedures for differential propagation phase shift. Preprints, *22nd Conf. on Radar Meteorology,* Zurich, Amer. Meteor. Soc., 397–399.

Pruppacher, H. R., and J. D. Klett, 1978: *Microphysics of Clouds and Precipitation.* D. Reidel, 714 pp.

Sachidananda, M., and D. S. Zrnić, 1986: Differential propagation phase shift and rainfall rate estimation. *Radio Sci.*, **21**, 235–247.

——, and ——, 1987: Rain rate estimated from differential polarization measurements. *J. Atmos. Oceanic Technol.*, **4**, 588–598.

——, and ——, 1989: Efficient processing of alternately polarized radar signals. *J. Atmos. Oceanic Technol.*, **6**(1), 173–181.

Seliga, T. A., and V. N. Bringi, 1978: Differential reflectivity and differential phase shift: Applications in radar meteorology. *Radio Sci.*, **13**(2), 271–275.

Ulbrich, C. W., 1983: Natural variations in the analytical form of raindrop size distribution. *J. Climate Appl. Meteor.*, **22**, 1764–1775.

——, and D. Atlas, 1984: Assessment of the contribution of differential polarization to improved rainfall measurements. *Radio. Sci.*, **19**, 49–57.

Zrnić, D. S., 1975: Simulation of weatherlike Doppler spectra and signals. *J. Appl. Meteor.*, **14**, 619–620.

——, 1979: Estimation of spectral moments for weather echoes. *IEEE Trans. Geophys. Sci. Electron.*, **GE-17**(4), 113–127.

——, N. Balakrishnan and M. Sachidananda, 1989: Polarimetric measurements determine the amounts of rain and hail in a mixture. Preprints, *24th Conf. Radar. Radar Met.*, Tallahassee, Amer. Meteor. Soc., 393–400.